A-5-1 (Invited)

Study of Dopant Diffusion and Defect Evolution for Advanced Ultra Shallow Junctions based on Atomistic Modeling

T. Noda[1], W. Vandervorst[2], S. Felch[3], V. Parihar[3], C. Vrancken[2], S. Severi[2], T. Y. Hoffmann[2], A. Falpin[2], B. van Daele[2], T. Jannssens[2], H. Bender[2], P. Eyben[2], M. Niwa[1], R. Schreutelkamp[3], F. Nouri[3], P. P. Absil[2], M. Jurczak[2], K. De Meyer[2], and S. Biesemans[2]

[1]Matsushita Electric Industrial Co., Ltd., 19 Nishikujo-kasugacho, Minami-ku, Kyoto 601-8413, Japan

Phone: +81-75-662-8993 E-mail: noda.taiji@jp.panasonic.com

[2]IMEC, Kapeldreef 75 B-3001, Leuven, Belgium

[3]Applied Materials, Sunnyvale, CA, USA

1. Introduction

Advanced ultra shallow junction (USJ) technologies are required for the 32 nm technology node and beyond. It is known that sub millisecond (ms) non-melt laser annealing (NLA), co-implant are a promising candidate [1-4]. In this work, study of dopant diffusion and defect evolution during advanced USJ is shown. An atomistic diffusion model is successfully used for the analysis of dopant diffusion.

2. Atomistic Modeling Approach

We use an atomistic kinetic Monte Carlo (KMC) diffusion model using DADOS [5] for the study of dopant diffusion and defect evolution. In our KMC model, the depth of amorphous layer and the solid phase epitaxial regrowth (SPER) velocity [6], which is important for accurate prediction of EOR defect behavior, is modified using experimental results. The geometry and binding energy for {311} defects and dislocation loops are considered. For the modeling of dopant activation/deactivation, the dopant-defect complexes, for instance, B_nI_m, As_nV_m are implemented. For the modeling of the fluorine (F) co-impact, Fluorine-vacancy complexes (F_nV_m) with different composition are implemented.

3. Results and Discussions

A. Spike + laser annealing: "+Laser" effect

"Spike-RTA + Laser" annealing is a bridging technology to combine the spike-RTA and sub-ms laser annealing. No additional diffusion during laser annealing after spike-RTA is shown. Figs. 1, 2 show the sheet resistance for F + B implant and As implant. It is shown that (1) "+Laser" becomes more effective with lower spike-RTA temperature (≤ 1010 ˚C), and (2) "+Laser" has a significant impact on As activation improvement. The Rs-Xj plot shows that "+Laser" is beneficial for As doped layers (Fig. 3). With the help of "+Laser", we can reduce the spike-RTA temperature and achieve shallower junctions. Fig. 4 shows an influence of absorbing layer (AL) is also quite important for the optimization of laser annealing sequence. However, pMOS exhibits very little improvement of Ion/Ioff due to "+Laser". Recently, we found that laser + spike-RTA sequence is also promising candidate for pMOS [3].

B. "Laser only" annealing process

Duing Partial amorphous regrowth at low temperature, B shows significant diffusion. B SIMS profiles show that B diffusion in the NLA process is 2-step diffusion (Fig. 5). Deeper PAI shows lower sheet resistance and low sensitivity to the laser peak temperature (Fig. 6). Fig. 7 shows KMC simulation results of sub-ms annealing at 1300 ˚C. KMC shows that after sub-ms annealing at 1300 ˚C, B_nI_m complexes are formed. Fig. 8 shows the B diffusivity extracted from SIMS profiles. B diffusivity in a-Si is higher than in c-Si at low temperature. However, during sub-ms annealing time range, B diffusivity in a-Si is lower than in c-Si in the higher temperature than 1100 ˚C.

C. EOR defect evolution during sub-ms annealing

Defect formation and evolution behavior during sub-ms annealing is an important topic for the junction leakage and junction thermal stability. EOR defects are clearly formed during sub-ms annealing time. The defect size is small and the defect density is very high. After 1300 ˚C NLA, {311} defects are still remaining and cannot transfer into the dislocation loops completely. Fig. 9 shows the KMC simulations of defect evolution during sub-ms annealing. KMC simulations also show that {311} defects cannot completely transfer into the dislocation loops at 1300˚C with sub-ms annealing. It is considered that the thermal budget of sub-ms annealing is too small for the full defect evolution.

D. F co-implant impact on sub-ms annealing

B SIMS profiles show that B-TED is increased as a function of F co-implant energy (Fig. 10). B diffusivity enhancement is observed at F co-implant energy higher than 5 keV. F SIMS profiles show that a large amount of F atoms are remaining inside the Si-substrate after sub-ms NLA. F can slow down SPER velocity [6]. We must conclude that B diffusivity is enhanced in c-Si in the presence of high concentration of F [8]. The lowest F implant energy shows an increase of sheet resistance (Fig. 16). There is a possibility that a fluorine-boron chemical interaction induces B deactivation [9]. KMC simulations with F_nV_m model show that in the presence of F, vacancy clusters remain in the Si-substrate after ms-annealing and form F_nV_m complexes (Fig. 11). This can explain the reason why much F remains in Si after sub-ms annealing. The presence of F_nV_m complexes enhances the EOR defect evolution and helps the EOR defect stability.

E. Advantage of sub-ms annealing in CMOS process

Fig. 12 shows the SSRM 2-dimensional carrier profiles. SSRM shows the NLA can reduce the both the depth and lateral direction. NLA can improve dopant activation level and suppress dopant TED. Therefore NLA device shows the reduction of S/D resistance and improved short channel effect.

4. Conclusion

NLA can improve the dopant activation dramatically and achieve shallow junctions. Our KMC model successfully used for the USJ analysis and it indicates that the thermal budget of sub-ms annealing is too small for full defect evolution, and one possible solution for defect stabilization is F co-implant. Consideration of the enhanced B diffusivity in a-Si is very important for accurate diffusion modeling of sub-ms annealing with pre-amorphous layer.

References

[1] S. Severi, *et al*., IEDM2006, p. 859 (2006). [2] T. Noda, *et al*., IEDM2006, p. 377 (2006). [3] T. Hoffmann, *et al*., IWJT2007, S8-3 (2007). [4] B. Pawlak, *et al*., APL, **89**, p. 062110 (2006). [5] M. Jaraiz, *et al*., MRS. Proc. **532**, p. 43 (1998). [6] G. Olson, *et al*., Mater. Sci. Rep. 3, p. 1 (1988). [7] T. Noda, *et al*., MRS Proc. **912**, C05-06 (2006). [8] T. Noda, *et al*., IIT2006 p. 21 (2006). [9] N. Cowern, *et al*., APL, **86**, p. 101905 (2005).

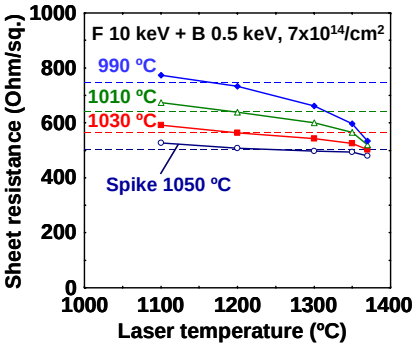

Fig. 1. Sheet resistance (Rs) of F + B co-implant with spike-RTA + Laser. Broken lines show Rs with spike-RTA.

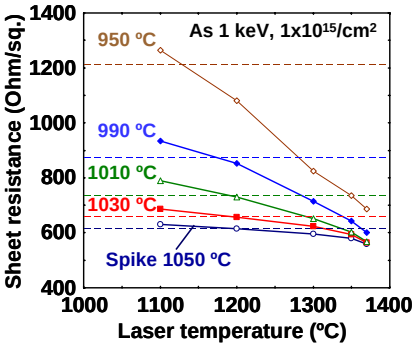

Fig. 2. Rs of As implant with spike-RTA + Laser. Broken lines show Rs with spike-RTA.

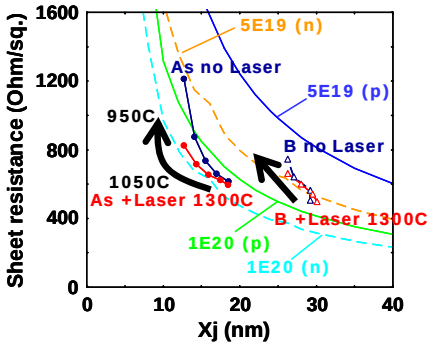

Fig. 3. Rs-Xj trade off plot for spike-RTA + Laser. Solid circle, open triangle is As, B data, respectively. Lines are ideal curve.

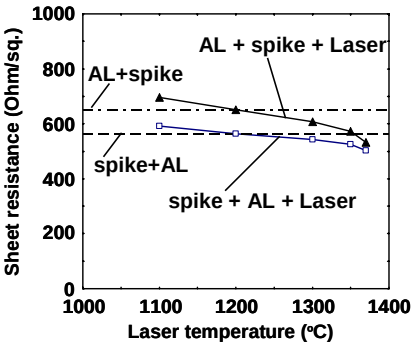

Fig. 4. Rs of F + B implant with spike-RTA + Laser. Absorbing layer (AL) sequences are compared. AL before spike-RTA increases Rs.

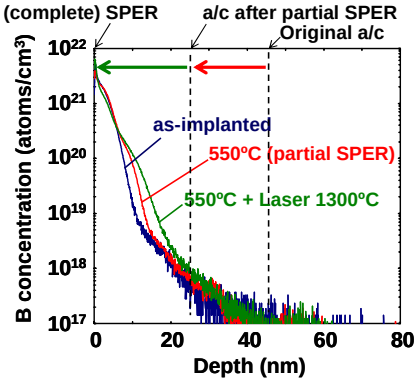

Fig. 5. B SIMS profiles during laser only annealing with partial SEPR. Ge 30 keV PAI + B 0.5 keV, $1x10^{15}/cm^2$ implant was used. Broken line shows the a/c interface.

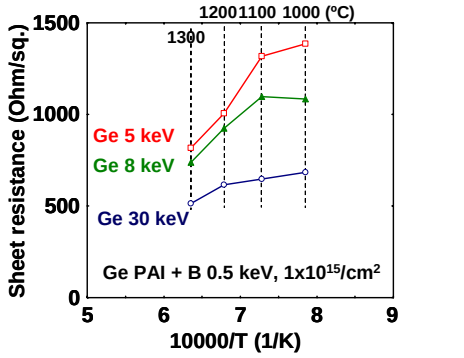

Fig. 6. Rs as a function of laser peak temperature with different Ge PAI energies.

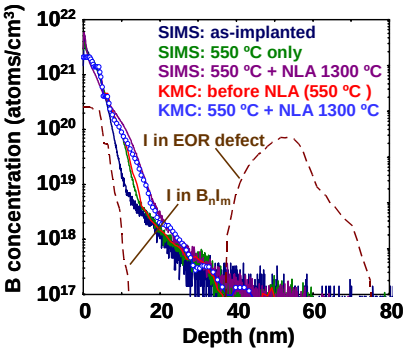

Fig. 7. Comparison between SIMS and KMC simulation for Laser only annealing at 1300 °C.

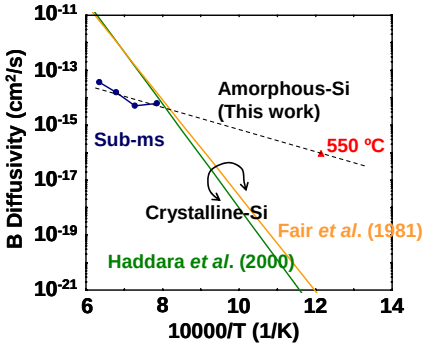

Fig. 8. B diffusivity in amorphous-Si.

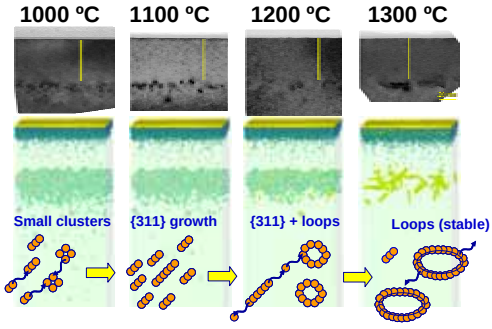

Fig. 9. KMC atomistic modeling of defect evolution of end-of-range defect.

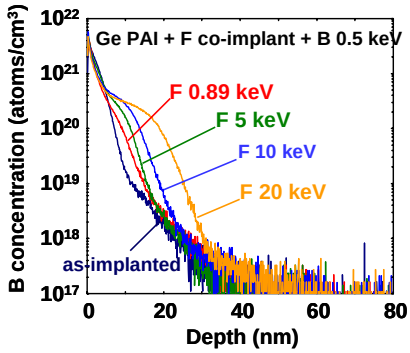

Fig. 10. B SIMS profiles after sub-ms laser annealing at 1300 °C with various F co-implant energies.

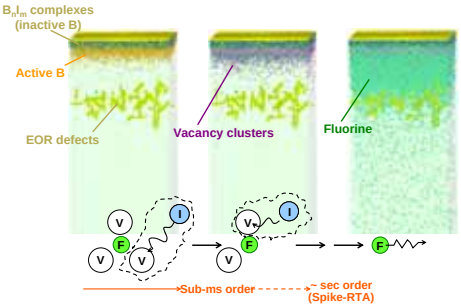

Fig. 11. KMC atomistic modeling of sub-ms annealing with F_nV_m model at 1300 °C.

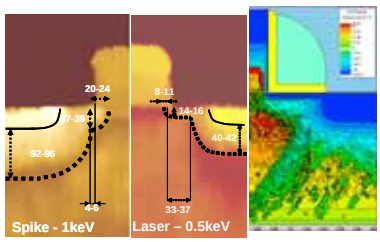

Fig. 12. Comparison between SSRM 2-dimentional carrier profiles and TCAD simulations. Spike-RTA data is also shown. (SSRM data: P. Eyben *et al*. MRS2006)